Inorg. Chem. **2004**, *43*, 8078–8084

Structure of the Amodiaquine–FPIX μ Oxo Dimer Solution Complex at Atomic Resolution

Angel C. de Dios,[†] Leah B. Casabianca,[†] Andrew Kosar,[†] and Paul D. Roepe*[,†,‡]

Department of Chemistry, Department of Biochemistry and Molecular Biology, and Program in Tumor Biology, Georgetown University, 37th and O Streets NW, Washington, D.C. 20057

Received July 26, 2004

Using NMR inversion recovery experiments and XPLOR distance restraint calculations, we recently deduced the structure of ferriprotoporphyrin IX (FPIX) heme μ oxo dimer–antimalarial drug complexes for chloroquine (CQ), quinine (QN), and quinidine (QD) at atomic resolution [A. Leed et al., *Biochemistry* **2002**, *41*, 10245–55]. Using similar methods, we now report an unexpected structure for the complex formed between FPIX and the related drug amodiaquine (AQ). The deduced structure is further supported by comparing AQ chemical-shift data to restricted Hartree–Fock calculations. The structure further highlights the critical nature of quinoline drug side-chain composition in stabilizing noncovalent association to FPIX. Heme Fe–AQ proton distances are longer, relative to those of the CQ complex, and the AQ aromatic side chain seems to have a significant role in stabilizing the complex. Relative to the FPIX–CQ complex, a similar 2:1 stoichiometry was determined for the AQ complex, in contrast to a 4:1 stoichiometry previously suggested from calorimetry data. These solution structures add to our rapidly growing understanding of the mechanism of quinoline antimalarial drug action and will help elucidate the mechanism(s) of quinoline antimalarial drug resistance phenomena.

Introduction

The continued spread of chloroquine resistance (CQR) greatly impedes the treatment of *P. falciparum* malaria, which kills millions annually. Additional drugs in development, and/or existing drug combinations, may offer some hope in treating CQR strains;[1] however, in most cases, there is a lack of tools for systematically inspecting drug−drug-target interactions at an atomic level, which makes preclinical antimalarial drug development particularly challenging. One well-studied, particularly useful class of antimalarial drugs are the quinolines (e.g., chloroquine (CQ), quinine (QN), mefloquine (MF), tafenoquine (TFQ), and amodiaquine (AQ)). The variable potency of these drugs is not understood at a molecular level, nor are cross-resistance patterns among these drugs for different drug-resistant strains of malaria. It is thus important to study how various quinoline antimalarials interact with their principal target(s). It has become increasingly evident that heme from hemoglobin (ferriprotoporphyrin IX (FPIX)), which is released upon enzymatic digestion of hemoglobin within the parasite digestive vacuole (DV), is a principal target of quinoline antimalarial drugs.[2] Elucidating these quinoline−heme interactions in detail is important for several reasons.

FPIX is a toxic byproduct of hemoglobin digestion, from which the parasite derives amino acids for rapid intraerythrocytic growth. Because malarial parasites lack the heme oxygenase pathway, FPIX is detoxified by sequestration into nontoxic crystalline hemozoin[3] within the parasite DV. Weak base quinoline antimalarials accumulate in the acidic DV and disrupt hemozoin formation via an as-yet incompletely understood mechanism. Several studies have provided data that suggest these drugs likely inhibit hemozoin crystallization (at least in part) by interacting with one or more forms of uncrystallized FPIX (i.e., either the FPIX monomer, the μ oxo dimer, or Fe−O41 reciprocal "head-to-tail" dimers).[4−8]

* To whom correspondence should be addressed. Telephone: (202) 687-7300. Fax: (202) 687-6209. E-mail: roepep@georgetown.edu.
[†] Department of Chemistry.
[‡] Department of Biochemistry and Molecular Biology, and Program in Tumor Biology.

(1) Dorsey, G.; Vlahos, J.; Kamya, M. R.; Staedke, S. G.; Rosenthal, P. J. *J. Infect. Dis.* **2003**, *188* (8), 1231−1238.
(2) Ursos, L. M. B.; Roepe, P. D. *Med. Res. Rev.* **2002**, *22* (5), 465−491.
(3) Pagola, S.; Stephens, P. W.; Bohle, D. S.; Kosar, A. D.; Madsen, S. K. *Nature* **2000**, *404* (6775), 307−310.
(4) Moreau, S.; Perly, B.; Biguet, J. *Biochimie* **1982**, *64* (11−12), 1015−25.
(5) Moreau, S.; Perly, B.; Chachaty, C.; Deleuze, C. *Biochim. Biophys. Acta* **1985**, *840* (1), 107−16.
(6) Constantinidis, I.; Satterlee, J. D. *J. Am. Chem. Soc.* **1985a**, *110* (3), 927−932.

10.1021/ic0489948 CCC: $27.50
Published on Web 11/06/2004

More recently, direct atomic level resolution of some drug−FPIX structures have become available and show that binding to multiple forms of FPIX is indeed possible for some drugs.[9,10]

Historically, several NMR techniques have been used to study antimalarial drug−FPIX interactions. Earlier studies used FPIX paramagnetic Fe line-broadening effects on proton[4,5] or carbon[6] resonances of CQ and QN to estimate drug−heme complex structures qualitatively. Despite the lack of angstrom-resolution models, these important studies suggested noncovalent association between drugs and FPIX μ oxo dimers in solution, with positive $\pi-\pi$ interactions between the quinoline aromatic rings and the FPIX tetrapyrrole. More recently, detailed inversion recovery experiments, followed by energy minimization calculations, have provided atomic-level resolution structures for some noncovalent drug−FPIX μ oxo dimer complexes formed in solution.[9] These studies used proton relaxation rates to explicitly calculate distances between protons of noncovalently bound antimalarial drugs and the FPIX Fe center. These experimentally derived distances then allowed energy minimization of the noncovalent bimolecular complexes via XPLOR.

Subtle differences in the structures of the complexes were observed upon protonation of the drugs. This indicated that small changes in the DV pH could, in theory, disrupt or strengthen the interactions between quinoline drugs and the μ oxo dimer FPIX.[9] This is particularly important because drug-resistant malaria parasites show altered DV pH.[11,12] The relative abundance of noncovalent complexes formed between some drugs and FPIX dimers, versus recently elucidated covalent complexes formed between these drugs and FPIX monomers,[10] remains to be determined. Yet, it is likely that some combination of these explains much of quinoline antimalarial pharmacology.

Amodiaquine (AQ) is an important aminoquinoline drug that is related to CQ. Early use of the drug was limited, because of toxic side effects,[13] but interest in the compound has recently been resuscitated because AQ has been shown (i) to have higher activity against some CQ-resistant strains and (ii) to have utility as a component of combination therapy.[1,14] Although its mode of action is believed to be similar to that of CQ, detailed analysis of its interaction with FPIX has not been conducted previously. In this paper, we elucidate the structural and energetic parameters of AQ−FPIX μ oxo dimer noncovalent association and compare them to those previously elucidated for CQ.[9] Key features of the deduced structure differ from the AQ−FPIX complex geometry modeled previously.[15] The data are relevant for drug design efforts and for deciphering the molecular basis of antimalarial drug resistance.

Materials and Methods

Materials. FPIX and AQ were obtained from Sigma (St. Louis, MO), and D_2O was obtained from Cambridge Isotope Laboratory (Andover, MA). Five-millimeter-diameter NMR tubes were purchased from Wilmad Glass Co., Inc. (Buena, NJ). All other reagents were analytical grade or better and purchased from commercial sources.

Sample Preparation. A 20 mM AQ stock solution was made in D_2O that had been buffered at pD 6.5. A 20 mM FPIX stock solution was made in dilute NaOH in D_2O. Solutions at variable AQ:FPIX ratios were mixed in 1.5-mL eppendorf tubes to a total volume of 1 mL under buffered conditions and then transferred to 5-mm NMR tubes and sealed. Paramagnetic relaxation effects were measured for multiple samples that titrated AQ (final concentration of 10 mM in all samples) versus increasing FPIX (final concentration of 0 mM to 0.4 mM in various samples).

NMR Spectroscopy and Molecular Modeling. All measurements were performed with a Varian Unity Inova 500 MHz NMR spectrometer, using Varian VNMR version 5.1 software. The temperature was maintained at 298 K throughout the experiments. For AQ proton peak assignments, ^{1}D proton NMR and double-quantum COSY were performed on a 10 mM AQ solution in the absence of FPIX. Measurement of the proton longitudinal relaxation times (T_1) and molecular dynamics calculations using XPLOR were done as previously described.[9] T_1 was measured via inversion recovery, using the classic pulse sequence: $180-\tau-90$.

Several assumptions related to electron-spin T_1 and binding kinetics are important in analyzing these spectra. For example, the effective correlation time is defined by via the relation ($1/t$ (effective)) = $1/t$ (rotation) + $1/t$ (exchange) + $1/t$ (electron relaxation). It is essentially equal to t (electron relaxation) = (2×10^{-12} s) for the following reasons. The rotational correlation time of the large FPIX dimer-drug complex will be on the order of $10^{-8}-10^{-9}$ s.[2] The exchange correlation time (binding and unbinding) is not diffusion-limited, because there is measurable binding energy and exchange occurs on a time scale of $>10^{-8}$ s.[3] We may neglect rotational and exchange contributions if the electron relaxation time is orders of magnitude shorter, as in this case.

Chemical-Shift Calculations. Chemical-shift calculations were performed on one of the low-energy structures obtained from the XPLOR calculations, with the Fe(III) in heme replaced by a closed-shell, diamagnetic Mg^{2+} ion. The side chains (ethylene and propionic acid) were also removed from the porphyrin and were replaced by H atoms. Chemical shifts were calculated using GIAO[16] with the hybrid functional B3LYP.[17,18] A 6-311G^{2d,2p} basis set[19] was used. Counterpoise corrections[20] were included, to correct for basis set superposition errors. The isotropic shielding of each

(7) Constantinidis, I.; Satterlee, J. D. *J. Am. Chem. Soc*. **1985b**, *110* (13), 4391−4395.
(8) Dorn, A.; Vippagunta, S. R.; Matile, H.; Jaquet, C.; Vennerstrom, J. L.; Ridley, R. G. *Biochem. Pharmacol*. **1998**, *55* (6), 727−736.
(9) Leed, A.; DuBay, K.; Ursos, L. M.; Sears, D.; De Dios, A. C.; Roepe, P. D. *Biochemistry* **2002**, *41* (32), 10245−55.
(10) de Dios, A. C.; Tycko, R.; Ursos, L. M. B.; Roepe, P. D. *J. Phys. Chem. A* **2003**, *107*, 5821−5825.
(11) Dzekunov, S. M.; Ursos, L. M.; Roepe, P. D. *Mol. Biochem. Parasitol*. **2000**, *110* (1), 107−124.
(12) Bennett, T. N.; Kosar, A. D.; Ursos, L. M. B.; Dzekunov, S.; Sidhu, A. B. S.; Fidock, D. A.; Roepe, P. D. *Mol. Biochem. Parasitol*. **2004**, *133*, 99−114.
(13) Naisbitt, D. J.; Ruscoe, J. E.; Williams, D.; O'Neill, P. M.; Pirmohamed, M.; Park, B. K. *J. Pharmacol. Exp. Ther*. **1997**, *280*, 884−893.
(14) Rwagacondo, C. E.; Niyitegeka, F.; Sarushi, J.; Karema, C.; Mugisha, V.; Dujardin, J. C.; Van Overmeir, C.; van den Ende, J.; D'Alesandro, U. *Am. J. Trop. Med. Hyg.* **2003**, *68* (6), 743−747.
(15) O'Neill, P. M.; Bray, P. G.; Hawley, S. R.; Ward, S. A.; Park, B. K. *Parmacol. Ther*. **1998**, *77* (1), 29−58.
(16) Ditchfield, R. *Mol. Phys.* **1974**, *27* (4), 789−807.
(17) Becke, A. D. *J. Chem. Phys.* **1993**, *98* (7), 5648−5652.
(18) Lee, C.; Yang, W.; Parr, R. G. *Phys. Rev. B* **1988**, *37* (2), 785−789.
(19) Hehre, W. J.; Radom, L.; Schleyer, P.; Pople, J. A. *Ab Initio Molecular Orbital Theory*; Wiley: New York, 1986.
(20) Boys, S. F.; Bernardi, F. *Mol. Phys.* **1970**, *19* (4), 553−566.

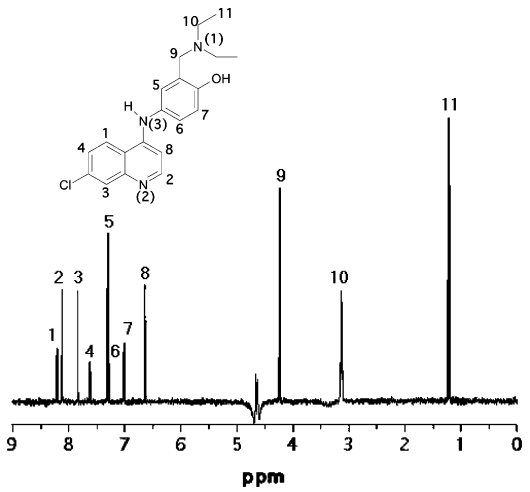

Figure 1. 1D NMR spectrum (10 mM AQ at pD 6.5) and chemical structure of AQ. Peaks were assigned using DQ-COSY.[24] Protons are labeled according to the position of their peaks in the 1D NMR spectrum. When more than one proton is assigned the same number, it indicates that these are chemically equivalent protons in solution. The different N atoms are also labeled in parentheses, according to their protonation order.

amodiaquine proton in the AQ−porphyrin complex was compared to the shielding calculated in an amodiaquine molecule with ghost orbitals located at the position of Mg-porphyrin atoms in the complex. The component of the overall change in chemical shift that is due to ring-current effects from the porphyrin ring was calculated by placing a neutron at each position where an amodiaquine proton would be located in the complex.[21] The neutron was used as a probe to determine the nucleus-independent chemical shift (NICS)[22] at each of these positions. The use of neutrons in place of the AQ atoms provides a way to calculate only the ring-current chemical shifts at those positions. This allows us to test whether most of the chemical shifts we calculate using a molecule of AQ with its nuclei and electrons are dominated by ring-current shifts, by comparing the results from the supermolecule versus the neutron calculations (see Discussion). All calculations were performed using the Gaussian 98 program[23] with four processors on a personal computer (PC) cluster at the University of Illinois at Chicago.

Results

Figure 1 shows the 1D proton NMR spectrum of 10 mM AQ in pD 6.5 buffered D_2O. Peak assignments follow the AQ proton numbering scheme that is also shown in Figure 1. To measure the longitudinal relaxation times (T_1) for individual AQ protons, inversion recovery experiments were conducted on AQ:FPIX mixtures ranging in molar stoichiometry from 1:0 to 25:1, with the AQ concentration remaining constant at 10 mM. Because of the solubility characteristics of AQ, these experiments were performed in pD 6.0 aqueous solution, where the μ oxo dimer form of FPIX predominates.[9] This is physiologically relevant, because the malarial parasite DV pH lies between 5 and 6.0.

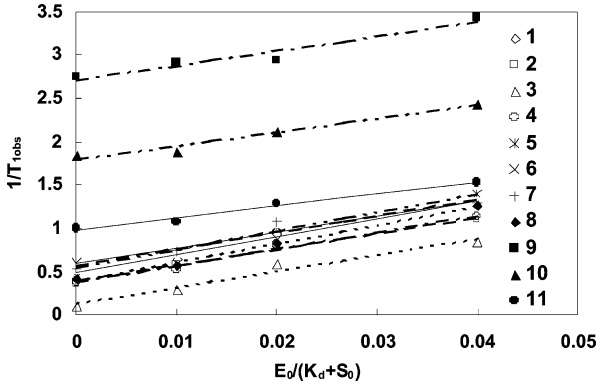

Figure 2. Plot of $1/T_1$ (observed) vs [FPIX]/(Kd + [AQ]) (see ref 9; E_0 = FPIX, S_0 = AQ). [AQ] is constant at 10 mM, while [FPIX] increases from 0 mM to 0.4 mM, causing a linear increase in the relaxation rate of the AQ protons. This linear relationship indicates a 1:1 stoichiometry between AQ and the FPIX μ oxo dimer, which is, by far, the dominant heme species under these conditions. AQ H−FPIX Fe distances (cf. Table 1) are calculated from the slope of the linear regression, using the Solomon−Bloembergen equation.[9]

As previously observed for other quinoline antimalarials,[9] increasing the FPIX concentration decreased the T_1 value of AQ protons (Figure 2), with quinoline protons (1, 4−8) being more sensitive to the paramagnetic effect, relative to side-chain protons. All T_1 plots were linear (see Figure 2), indicating a 1:1 drug:FPIX dimer stoichiometry at these concentrations of AQ, similar to the case previously described for CQ.[9] This is likely a consequence of rapid equilibrium between noncovalent AQ association and hydroxyl axial ligands at each face of the dimer.[6,9] Slopes of these T_1 vs [FPIX] plots were used to calculate distances between AQ protons and FPIX Fe via the Solomon−Bloembergen equation.[9] Table 1 presents the measured distances for the diprotic (2+) species of AQ (column 1) and compares them to distances computed after XPLOR energy minimization of the complex (see below). There was excellent agreement (<1.0 Å) between computed and measured distances. Considering the pK_a value of AQ and the known DV pH, it is unlikely that any form of AQ other than diprotic AQ (AQ 2+) binds to FPIX within the malarial parasite DV. Overall, AQ H/FPIX Fe distances are greater than the corresponding CQ H/FPIX Fe distances measured earlier.[9] The greater overall distances, relative to CQ, are consistent with relatively lower AQ−heme association constants that have been measured previously.[8]

With the T_1 distance constraints in hand, XPLOR energy minimization was used to generate a set of 28 AQ−FPIX complex structures, as previously described.[9] All solutions were consistent with the distance constraints imposed by the inversion recovery data, as well as known bond angles, bond lengths, etc.[9] These complex structures had remarkably

(21) Wolinski, K. *J. Chem. Phys.* **1997**, *106* (14), 6061−6067.
(22) Schleyer, P. v. R.; Maeker, C.; Dransfeld, A.; Jiao, H.; Hommes, N. J. R. v. E. *J. Am. Chem. Soc.* **1996**, *118* (26), 6317−6318.
(23) Frisch, M. J.; Trucks, G. W.; Schlegel, H. B.; Scuseria, G. E.; Robb, M. A.; Cheeseman, J. R.; Zakrzewski, V. G.; Montgomery, J. A., Jr.; Stratmann, R. E.; Burant, J. C.; Dapprich, S.; Millam, J. M.; Daniels, A. D.; Kudin, K. N.; Strain, M. C.; Farkas, O.; Tomasi, J.; Barone, V.; Cossi, M.; Cammi, R.; Mennucci, B.; Pomelli, C.; Adamo, C.; Clifford, S.; Ochterski, J.; Petersson, G. A.; Ayala, P. Y.; Cui, Q.; Morokuma, K.; Malick, D. K.; Rabuck, A. D.; Raghavachari, K.; Foresman, J. B.; Cioslowski, J.; Ortiz, J. V.; Stefanov, B. B.; Liu, G.; Liashenko, A.; Piskorz, P.; Komaromi, I.; Gomperts, R.; Martin, R. L.; Fox, D. J.; Keith, T.; Al-Laham, M. A.; Peng, C. Y.; Nanayakkara, A.; Gonzalez, C.; Challacombe, M.; Gill, P. M. W.; Johnson, B. G.; Chen, W.; Wong, M. W.; Andres, J. L.; Head-Gordon, M.; Replogle, E. S.; Pople, J. A. *Gaussian 98*, revision A.7; Gaussian, Inc.: Pittsburgh, PA, 1998.
(24) Rance, M.; Sørensen, O. W.; Bodenhausen, G.; Wagner, G.; Ernst, R. R.; Wüthrich, K. *Biochem. Biophys. Res. Commun.* **1983**, *117* (2), 479−485.

Table 1. Average AQ H−FPIX Fe Distances for the Diprotic Drug Complexed to FPIX μ-oxo Dimer[a]

	Mean H−Fe and N−Fe Distances (Å)	
atom	measured	calculated
H1	5.33	5.49 (0.27)
H2	5.46	6.24 (0.17)
H3	5.45	6.42 (0.08)
H4	5.41	6.35 (0.15)
H5	5.48	5.27 (0.29)
H6	5.42	4.96 (0.64)
H7	5.31	4.98 (0.67)
H8	5.31	5.80 (0.32)
H9	5.41	6.24 (0.40)
H10	5.51	5.27 (0.89)
H11	5.67	6.03 (0.76)
N1		5.31 (0.39)
N2		5.30 (0.37)
N3		5.68 (0.11)

[a] Distances are tabulated for both NMR-derived and XPLOR-minimized values of AQ. Note the excellent agreement, validating the XPLOR approach, as described previously.[9] [b] Values given in parentheses represent the standard deviation.

similar energies, varying from 198 to 240 kcal/mol (data not shown). Figure 3 shows side (Figure 3A) and axial (Figure 3B) views of the geometries for a representative set of these AQ−FPIX complexes. For clarity, the second FPIX in the μ oxo dimer molecule (which is attached to the first via an almost-linear Fe−O−Fe bond) is not shown. In these superimposed structures, the AQ quinoline ring was fixed and all other atoms were allowed to arrange themselves accordingly. This highlights the flexible features of the noncovalent AQ−FPIX structure versus those that are relatively fixed. As observed from the axial view (Figure 3B), the quinoline ring is not directly above the Fe center, as previously suggested,[4,5] but lies toward the side of the FPIX tetrapyrrole, presumably to optimize favorable $\pi-\pi$ interactions. This is somewhat similar to previous observations for CQ, QN, and QD complexes.[9] However, unlike CQ, QN, and QD, flexible side-chain wrapping that follows the periphery of FPIX is more limited for AQ (Figure 3). Unlike CQ, the entire AQ side chain traverses the FPIX macrocyle and maintains a relatively fixed geometry. Presumably, this is to accommodate additional $\pi-\pi$ stabilization of the complex afforded by the aromatic side-chain moiety. That is, the presence of the aromatic group in the AQ side chain limits side-chain flexibility and further stabilizes the complex with an added $\pi-\pi$ interaction versus the opposite side of the FPIX tetrapyrrole. Notably, despite the inclusion of explicit electrostatic interactions in the XPLOR calculations, no ionic interactions (through the AQ NH^+ and the FPIX COO^-) are observed. This is in contrast to previously suggested AQ−FPIX complex models[15] that were not refined via explicit, experimentally derived drug H−FPIX Fe distances, as is the case here.

The side view (Figure 3A) shows how the quinoline and side-chain planes are positioned, relative to the FPIX plane. As previously described for diprotic QN and QD,[9] we find that the angle between the FPIX plane and the short axis of the AQ quinoline ring is decidedly nonzero (a mean value of 34° was determined for the 28 XPLOR structures). Similarly, the side-chain ring is tilted ~32°, relative to the

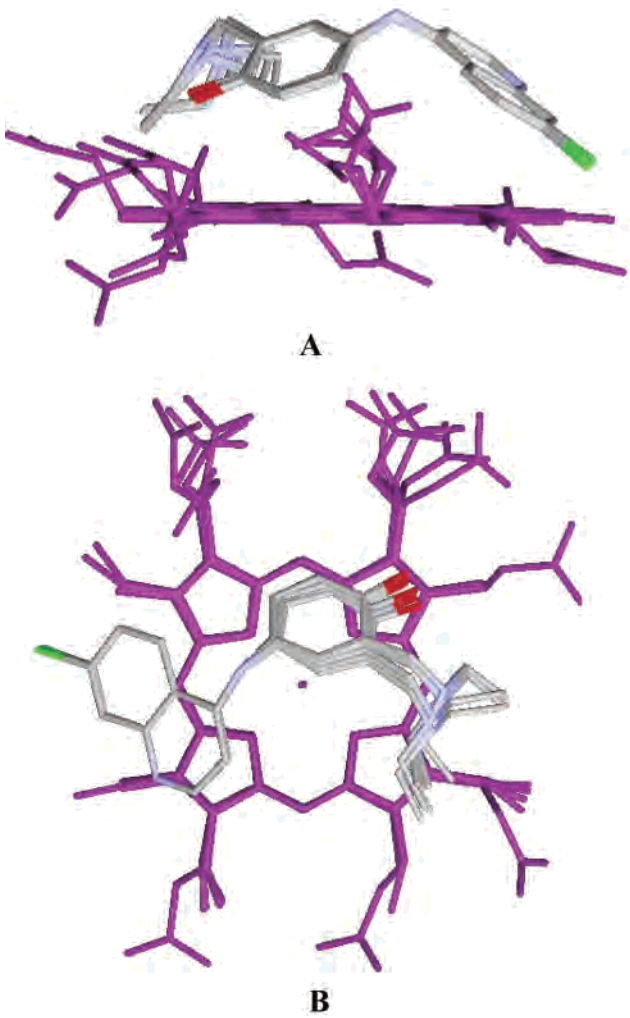

Figure 3. (A) Side view and (B) axial view of the lowest-energy structures for AQ complexed with FPIX μ oxo dimer. Protons and the second FPIX moiety of the μ-oxo dimer are omitted for clarity. The structures are superimposed such that the quinoline rings for multiple XPLOR solutions consistent with NMR distance constraints are exactly overlapped and the rest of the drug and FPIX atoms are allowed to arrange themselves accordingly (to illustrate flexibility of the complex).

FPIX plane. Thus, in the series of four quinoline antimalarials for which we have solved FPIX structures to date (AQ, QN, QD, CQ), only diprotic CQ forms an almost-coplanar arrangement with FPIX (see ref 9). Complexes formed with the other three quinoline drugs deviate significantly from coplanarity. For QN and QD, these interplanar angles were proposed to exist (in part) because of repulsion between the QN and QD OH groups and the FPIX Fe. For AQ, the situation is different. We suggest geometry about the anilinal−type N (including a lone pair of electrons) influences the available conformations that can be sampled by AQ as it optimizes $\pi-\pi$ interaction with FPIX. Another contribution to this geometry is likely repulsion between the aliphatic N (N1), the quinoline N (N2), and the FPIX Fe. Repulsion would act to optimize the sum of the distances between the positive Fe center of FPIX and the protonated N.

We also observed subtle changes in the chemical shift of AQ protons as the AQ:heme ratio was decreased (Table 2).

Table 2. Experimental and Calculated Change in Chemical Shift of Each Proton as AQ Complexes to Heme, and the Component of This Change that Is due to Ring-Current Effects from the Heme Porphyrin Ring[a]

	Change in Chemical Shift		
proton	experimental	calculated	ring current
1	−0.6470	−1.7623	−1.8844
2	0.2023	−1.0387	−0.9411
3	−0.1494	1.0575	1.0783
4	−0.7041	0.0154	0.1722
5	−1.6426	−2.5591	−2.5062
6	−1.3352	−3.4447	−3.6008
7	−2.2788	−2.4362	−3.2274
8	−0.1255	−1.9378	−1.9744
9	−0.7385	−1.5826	−1.5243
10	−0.4321	−2.0938	−2.6216
11	−0.1610	0.0047	−0.0956

[a] A positive number in each case means that the proton is more deshielded in the complex than in pure amodiaquine.

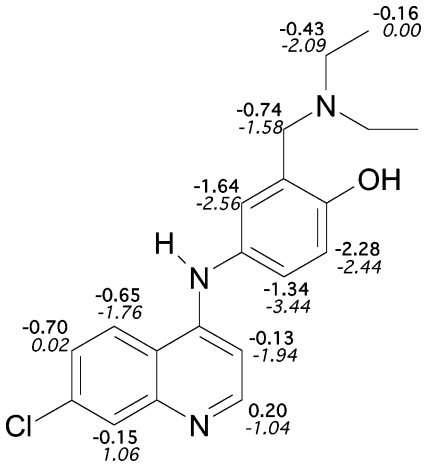

Figure 4. Experimental changes (bold font) and calculated changes (italic font) in the chemical shift of each AQ proton.

The experimental chemical shift of each amodiaquine proton in the AQ−FPIX complex was extrapolated from plots similar to how T_1 values for the complex were determined, as shown in Figure 2. Column 1 of Table 2 contains the experimental change in chemical shift for each proton, which is the extrapolated chemical shift of each proton in the AQ−FPIX complex minus the chemical shift in pure AQ. In comparing proton chemical shifts for the AQ−FPIX complex versus pure AQ, we note that all but one of the protons becomes more shielded when AQ complexes to FPIX heme. Also, protons on one face of the drug molecule are more shielded than those on the other, which is consistent with the arrangement of AQ protons versus FPIX, as shown in Figure 3. In addition, protons on the phenol ring have larger changes in chemical shift than protons on the quinoline ring. This is because the phenol protons are closer to the Fe atom and to the porphyrin ring.

To investigate the nature of these chemical shifts, we performed B3LYP level chemical-shift calculations using a 6-311G (2d, 2p) basis set. The calculated change in chemical shift (the calculated isotropic shielding of each proton in AQ with counterpoise corrections minus the shielding in the AQ−heme complex) for each AQ proton is listed in column 2 of Table 2. These values are the same order of magnitude as the experimental changes in chemical shift and show similar trends. Most of the protons become more shielded as AQ complexes to heme, and protons on the phenol ring have a larger change in chemical shift than protons on the quinoline ring. Figure 4 shows the experimental changes (bold font) and calculated changes (italic font) in chemical shift that are superimposed on the structure of AQ.

The nucleus-independent chemical shift[22] was calculated for each proton by performing a chemical-shift calculation in which the AQ molecule in the AQ−FPIX complex was replaced by neutrons at each position where an AQ proton would be located.[21] Electrons and other nuclei in the AQ molecule were removed; however, the heme molecule was unmodified. The neutrons report a shielding that is due only to ring-current effects from the heme porphyrin and is independent of any influences from other nuclei or electrons in the AQ molecule. These results are presented in column 3 of Table 2. These changes are the same order of magnitude as the experimental changes in chemical shift and are in excellent agreement with the calculated changes in chemical shift.

Discussion

Rapidly mounting evidence strongly suggests that quinoline antimalarial drugs are toxic to malarial parasites via interactions with noncrystalline FPIX heme released within the malarial parasite DV.[2] However, the molecular details of these interactions are not yet fully elucidated. Such information is essential for understanding the pharmacology of these drugs, as well as for drug design that will hopefully keep pace with quinoline antimalarial drug resistance.[2] This study presents the first solution structure of the AQ−FPIX μ oxo dimer complex at atomic resolution. Conditions of this study favored the presence of the soluble FPIX μ oxo dimer. We note that this dimer may or may not be the only heme species relevant for quinoline antimalarial pharmacology. It has also recently been shown that acid pH and vastly substoichiometric addition of antimalarial drugs can promote the aggregation of FPIX,[11,25] and also that some quinoline antimalarials may form covalent complexes with monomeric FPIX.[10] Measurement of the relative concentrations of different possible FPIX species (FPIX monomer, μ-oxo dimer, Fe−O41 dimer, and their aggregates) present in vivo are needed to completely understand the pharmacologic importance of these various complexes.

Nonetheless, the FPIX μ oxo dimer is predicted to be a major component of DV heme pools.[2] Importantly, the present study illustrates how noncovalent AQ−FPIX dimer interactions differ from those of CQ, QN, and QD[9] and, thus, add significantly to the "basis set" of structural principles for quinoline pharmacology. For example, it is notable that we now know that none of four different diprotic quinoline antimalarials form salt bridges with ionized FPIX propionic acid carboxylates. These ionic interactions have been commonly anticipated and discussed at length in the antimalarial

(25) Ursos, L. M.; DuBay, K. F.; Roepe, P. D. *Mol. Biochem. Parasitol.* **2001**, *112* (1), 11−17.

drug development literature (e.g., see O'Neill et al.[15] and references within). Yet, they appear irrelevant for stabilizing noncovalent FPIX−drug complexes. A combination of effects are likely responsible for reducing the significance of these potential ionic interactions. These include how the various complexes both optimize $\pi-\pi$ interactions and limit FPIX Fe−drug N repulsions, and also how they have a tendency to maximize entropy for the FPIX dimer.[9]

Similar to CQ, we find the AQ−FPIX complex exhibits a 1:2 stoichiometry (1 AQ per 1 FPIX μ-oxo dimer). This is in contrast to the previous 1:4 stoichiometry (1 AQ per 2 μ-oxo dimers) reported by Dorn et al.[8] The stoichiometry that we derive comes from equilibrium solution measurements, whereas earlier estimates were based on scanning calorimetry data that used FPIX samples in a semi-solid state. Further study of this interesting dichotomy is warranted; perhaps interaction in the solid state is not analogous to that in solution. Both may be relevant in vivo, depending on the exact value of the DV pH.[12]

CQ and AQ are both aminoquinolines, but they have very different side-chain compositions. Our previous results for CQ show that distances between the quinoline protons and the FPIX Fe range from 3.845 Å to 4.914 Å, whereas those for AQ (Table 1) range from 5.31 Å to 5.45 Å. This predicts that CQ has a higher affinity for FPIX than AQ. Lower affinity of AQ for FPIX predicted from these structures is indeed consistent with previous direct measurements of K_D.[8] In contrast, side-chain proton distances for both AQ and CQ generally are 5−6 Å. That is, although quinoline proton distances for CQ are ∼1 Å shorter than side-chain proton distances, the two are similar for AQ. The presence of an aromatic group in the AQ side chain, which seems to additionally stabilize the complex via $\pi-\pi$ interaction with the FPIX tetrapyrrole, biases the geometry of the AQ complex. Also perhaps adding to the stability of the AQ complex is the ability of the positive Fe center on the FPIX to interact with the superimposed electron lone pair on the anilinic N.

It is also noteworthy that, among AQ, QN, QD, and CQ, only diprotic CQ shows a co-planar noncovalent structure with FPIX. Interplanar angles of 20°−35° are actually much more common among this series of drugs. The angles seem to be reinforced by geometry constraints imposed by QN/QD hydroxyls or the AQ anilinic N. This is perhaps the most surprising (and potentially important) conclusion for future quinoline antimalarial drug design. That is, designing optimized co-planar drug−FPIX interactions may not be as beneficial (or necessary) as initially thought; rather, "puckered" interplanar geometries seem to be perfectly acceptable, if not favored. Much is yet to be learned about how $\pi-\pi$ interactions are optimized for various noncovalent bimolecular complexes. For example, non-obvious (nonplanar) geometries similarly have been observed recently for simple substituted benzene systems, wherein interplanar distance and geometry is significantly affected by aromatic substituents.[26]

(26) Sinnokrot, M. O.; Sherrill, C. D. *J. Phys. Chem. A* **2003**, *107* (41), 8377−8379.

Therefore, aside from the obvious importance with regard to antimalarial drug design, the AQ−FPIX structure reported here, when considered with previous noncovalent structures solved for CQ, QN, and QD vs FPIX,[9] forms another interesting experimental test case for further elucidating noncovalent $\pi-\pi$ interaction principles.

The chemical-shift studies provide additional insight into the nature of the AQ−FPIX complex formed in solution. The calculations are performed with the paramagnetic Fe^{3+} ion in heme being replaced by a Mg^{2+} ion, which is diamagnetic. If a covalent bond were formed between heme Fe and AQ quinolinal N in the complex, the experimental changes in chemical shift would be considerably larger than the calculated changes, because of contact hyperfine shifts.[10] These shifts result from through-bond spin delocalization of the unpaired Fe electrons and are absent in our calculations. Substantial changes in chemical shifts are not observed experimentally. Rather, the experimental changes are of the same order of magnitude as the calculated changes. Thus, contact hyperfine shifts are not responsible for the chemical-shift changes that we have observed.

Instead, because there is good correspondence between data and the neutron calculations, we suggest the observed changes in chemical shift are due primarily to ring-current effects. The ring-current contribution to the change in chemical shift was investigated by calculating the NICS at the position of the nucleus of interest.[21] Changes in chemical shift due to porphyrin ring-current effects were calculated for each AQ proton. Notably, these values are similar to the overall calculated change in chemical shift, indicating that the majority of the change is likely due to ring-current effects. The absence of hyperfine shifts and the agreement between the ring-current contribution and the overall change in chemical shift provide further evidence that the AQ−FPIX complex formed in solution is a noncovalent $\pi-\pi$ complex.

Proton chemical shifts are quite difficult to predict quantitatively. Full quantitative agreement is not expected at this level of theory for a highly dynamic and complex structure. To predict the proton shifts more quantitatively, electron correlation may be required, using the FPIX dimer combined with molecular dynamics that will time-average the shifts. The model used makes use of a Mg^{2+} complex to avoid performing an unrestricted Hartree−Fock calculation. Thus, the model will not include mild contributions from the unpaired electron spin (pseudo-contact shifts), if these are present. Nonetheless, because our calculations yield values that are of the same order of magnitude as the experimentally extrapolated shifts, we can conclude that most of the proton chemical-shift changes are due to the porphyrin ring (as in ring currents) and not the paramagnetic FPIX dimer.

It is also interesting to note that the protons for which the calculated and experimental changes in chemical shift are not of the same sign (protons 2, 3, and 4) also show the greatest disagreement between experimental and XPLOR-derived H−Fe distances (cf. Table 1). One source of error in determining the precise structure at better than 1.0 Å resolution is that the measured distance restraints are defined

from a single point, namely, the FPIX heme Fe. Because of the rapid relaxation afforded by the paramagnetic center, heme protons cannot be seen in solution NMR, and, therefore, NOE distances between FPIX and AQ protons are unfortunately not available. Because only distances from a single point are available, the AQ molecule could, in theory, be rotated about an axis through the Fe atom and perpendicular to the porphyrin ring, yet still satisfy all distance constraints defined by the inversion recovery experiments (within ± 1 Å). The effect of rotation about this axis was examined by rotating the FPIX molecule, keeping the Fe−H distances constant and then calculating the NICS of the AQ protons at these different orientations. Interestingly, no significant changes in the NICS were observed upon rotation of the heme molecule, indicating that ring-current effects on AQ chemical shifts are relatively independent of the orientation of AQ, with respect to FPIX about this rotation axis. Again, elucidating features of CQ, QN, QD, and AQ−FPIX complexes formed in solution may not only be critical for antimalarial drug development, but may also be of general use for understanding the chemistry of bimolecular complexes stabilized by $\pi-\pi$ interactions.

Acknowledgment. This work was supported by the NSF and the NIH (RO1 AI45957 to P.D.R.). We thank the Department of Chemistry at Georgetown and the University of Illinois at Chicago for additional computer resources, and Prof. Cynthia Jameson and Dr. Devin Sears (University of Illinois) for helpful conversations.

IC0489948